Insights on Resistance to Reverse Transcriptase: The Different Patterns of Interaction of the Nucleoside Reverse Transcriptase Inhibitors in the Deoxyribonucleotide Triphosphate Binding Site Relative to the Normal Substrate

Alexandra T. P. Carvalho, Pedro A. Fernandes, and Maria J. Ramos*

REQUIMTE, Departamento de Química, Faculdade de Ciências, Universidade do Porto, Rua do Campo Alegre, 687, 4169-007 Porto, Portugal

Received June 9, 2006

It is presently known that the long-term failure in the treatment of AIDS with the currently available nucleotide reverse transcriptase inhibitors (NRTIs) is related to the development of resistance by reverse transcriptase (RT) at the binding or incorporation level or both, or subsequent to the nucleotide incorporation (excision). To achieve greater insight on the differential interactions of two NRTIs that are mainly discriminated by different mechanisms, 2′,3′-didehydro-2′,3′-dideoxythymidine-5′-triphosphate (d4TTP, that is, phosphorylated stavudine) and 2′,3′-dideoxycytidine-5′-triphosphate (ddCTP, that is, phosphorylated zalcitabine), with the primer/template (p/t) and with the N binding site of reverse transcriptase (RT) in relation to the normal substrate (dNTP), we have conducted a series of molecular dynamics (MD) simulations. We propose that the different resistance profiles arise from the different conformations adopted by the inhibitors at the N site. d4TTP adopts an ideal conformation for catalysis because it forms an ion−dipole intramolecular interaction with the β-phosphate oxygen of the triphosphate, as does the normal substrate. In ddCTP, the lack of this essential interaction results in a different, noncatalytic conformation.

Introduction

The replication of human immunodeficiency virus (HIV) in infected cells relies on reverse transcriptase (RT). RT synthesizes a double-stranded DNA from the viral (+)-RNA genome suitable for integration in the host genome.[1]

Nucleotide reverse transcriptase inhibitors (NRTIs) are currently used clinically to inhibit retroviral replication. After conversion to the triphosphate active forms, the analogues compete with the normal substrates for binding and incorporation into the viral chain. Currently, the NRTIs zidovudine (AZT), staduvine (d4T), zalcitabine (ddC), didanosine (ddI), lamivudine (3TC), abacavir (ABC), emtricitabine (FTC), and tenofovir disopropil fumarate (TDF) have been approved by the US Food and Drug Administration and by the European Medicines Agency for HIV treatment. These prodrugs have a hydroxylated 5′ carbon and are subsequently phosphorylated by the cellular kinases to generate the active triphosphorylated form.

Antiretroviral drug resistance is an important limitation in treatment of HIV/acquired immunodeficiency syndrome (AIDS). Resistance mutations to NRTIs can emerge spontaneously because of the error prone replication of HIV-1.[2] The pattern of mutations developed by RT depends on the drugs administered during the antiretroviral therapy. Patients treated with AZT display a set of up to six mutations in the *pol* gene involving Met41Leu/Asp67Asn/Lys70Arg/Leu210Trp/Thr215Phe or Thr215Tyr/Lys219Gln, which are called thymidine analog mutations (TAMs); these mutations confer a >100-fold HIV-1 resistance to AZT. Regarding d4T, when it is given as the only drug to patients naive to AZT, RT bearing a Val75Thr substitution is selected in 10% of the cases.[3] However, the most important d4T resistance mutations are TAMs.[4] Resistance to ddC, ddI, and 3TC are conferred by single mutations in the *pol* gene, namely Lys65Arg,[5,6] Leu74Val,[7] and Met184Val;[8−10] furthermore, cases of multinucleoside and cross resistance exist such as the Gln151Met resistance complex [for a review, see Carvalho et al., *Mini.-Rev. Med. Chem.* **2006**, *6*, 549−555].[11]

There are two main mechanisms by which drug resistance mutations cause reduced viral susceptibility to NRTIs. The first mechanism, discrimination, affects the affinity and or incorporation of the analogue relative to the normal substrate; the second is the excision mechanism.[12−15] Excision is the reversal of polymerization and involves nucleophilic attack by a pyrophosphate donor (ATP or PPi) on the blocked primer with concomitant elimination of the bound NRTI, which permits DNA synthesis to continue.[16,17] ATP is believed to be the main pyrophosphate donor *in vivo*.[18−25] This mechanism was identified as the one responsible for resistance to both AZT and d4T.[16,17,24,26]

Several studies using RT bearing resistance mutations pointed out that the resistance mutations do not confer new properties to the mutant enzyme but, rather, exacerbate pre-existing properties of the wild-type (WT0 enzyme toward a given inhibitor.[6,13,16,17,23,24,26−30] Consequently, the pathway by which RT will evolve to become resistant toward a given inhibitor can be predicted by studying the inhibition of WT RT by this inhibitor.[31]

In this work, we are interested in investigating the structural determinants in the NRTI that cause RT resistance. Accordingly, we have conducted MD simulations of the WT RT·primer/template (p/t)·dTTP, RT·p/t·ddCTP, and RT·p/t·d4TTP complexes and compared the results obtained with the substrate and with the inhibitors (see Figure 2).

Even though resistance to ddC and d4T is caused by different types of mutations, they are structurally similar, both pyrimidine analogues, with hydrogens at the 3′-position of the ribose moiety (Figure 1). The only subtle difference is that the 3′-carbon of

* To whom correspondence should be addressed. Phone: +351 22 60 82 806. Fax: +351 22 60 82 959. E-mail: mjramos@fc.up.pt.

10.1021/jm060698c CCC: $33.50
Published on Web 12/05/2006

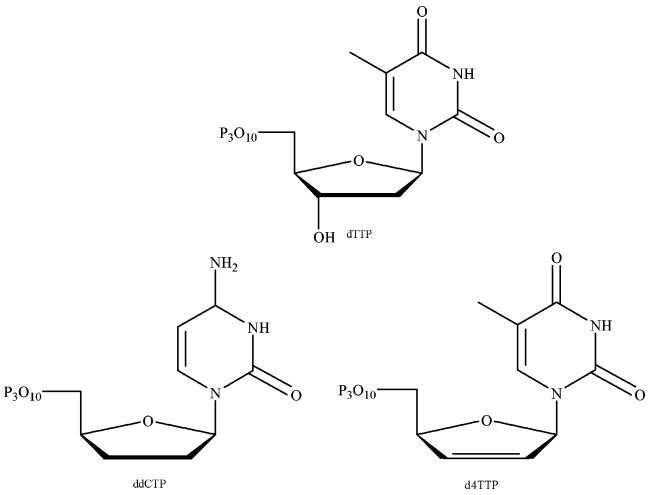

Figure 1. Structure of the normal substrate (dTTP) and of the analogues ddCTTP and d4TTP.

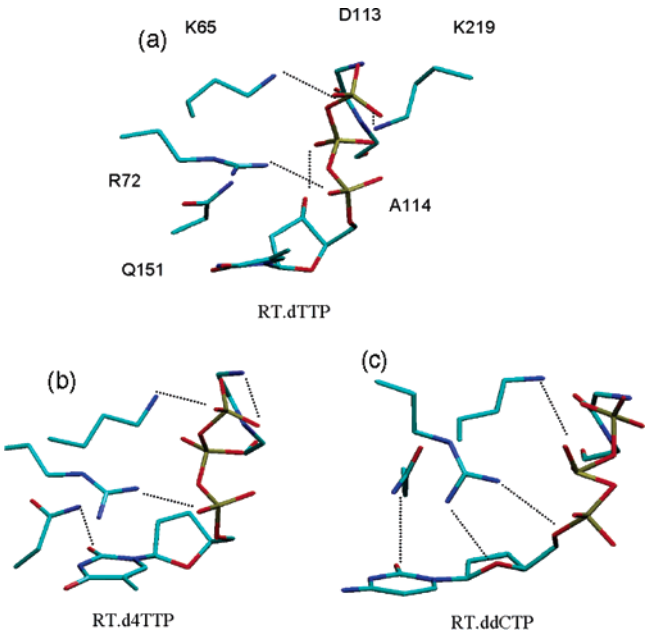

Figure 2. Residues in the dNTP binding site that interact with (a) the dNTP and with the inhibitors, (b) d4TTP and (c) ddCTP. The pattern of hydrogen bridges is different between the two inhibitors. d4TTP establishes interactions with the enzyme similar to the normal nucleoside. The structures were taken from the last picoseconds of simulation.

d4T has sp^2 hybridization but the 3′-carbon of the ddC has sp^3 hybridization.

With the simulations of the mentioned complexes, we were able to find an explanation for the discrimination mechanism at the level of incorporation. The nature of the group at the 3′-position of the ribose is the principal determinant for discrimination.

Results

1. Enzyme−p/t−Substrate/Inhibitor Interactions. To begin with, an analysis of the hydrogen bridges was made (Table 1, Figure 2), with the purpose of understanding the differential interactions of the inhibitors versus normal nucleotide in the dNTP binding site of WT RT. In the X-ray structure of the complex RT·p/t·dNTP (pdb code 1RTD),[32] we can see that the most important interactions of the triphosphate moiety of the nucleoside are established with Lys65, with Arg72, with the main chain NH groups of residues 113 and 114, and with two

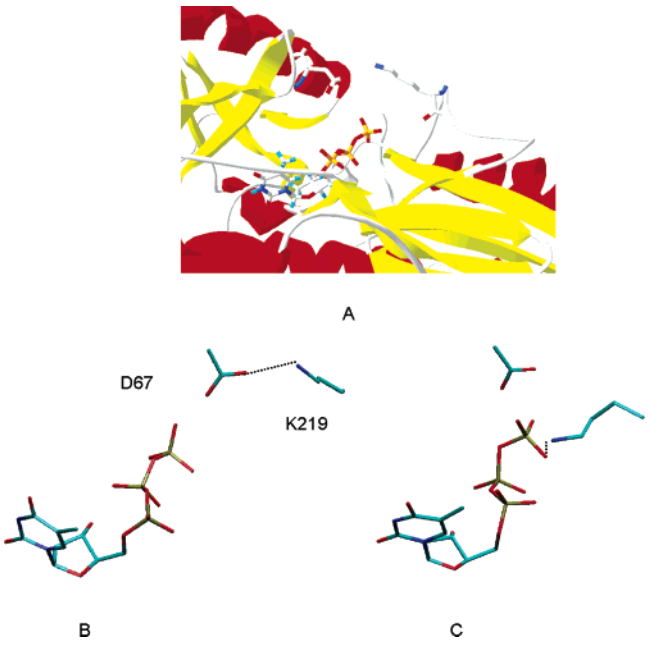

Figure 3. Panel A shows that Lys219 and Asp67 are located in the surface of RT in the entrance of the proposed ATP binding site. Panel B shows the position of Lys219 and Asp67 in the X-ray structure 1RTD. In panel C, during the simulation when the constraints are relieved, Lys219 moves toward the triphosphate of the dNTP.

metal ions (Mg^{2+}). The 3′-OH of dTTP enters into a small pocket defined by the side chains of Asp113, Tyr 115, Phe 116, and Gln 151 and the peptide backbone between 113 and 115. The simulation of the E·p/t·dNTP complex correctly reproduces the same pattern of hydrogen bridges between the triphosphate and the enzyme as in the X-ray structure (Figure 2, Table 1). However, the simulation also revealed a hydrogen bridge established between one oxygen of the γ-phosphate and Lys219 that is not present in the original X-ray structure.

2. Influence of Lys219 and Asp67 in Excision. In the X-ray structure, Lys219 is located at the surface of the protein, highly exposed, establishing a salt bridge with the also highly exposed fingertip residue, Asp67. The Lys219 N is 10.43 Å away from the γ-phosphate of the dNTP. During the simulation, the positively charged side chain of Lys219 is attracted to a negatively charged γ-phosphate oxygen and engages in an ionic hydrogen bridge with it. It is important to mention that even though Lys219 is attracted to the triphosphate, it maintains the salt bridge with the fingertip residue Asp67 (see Figure 3). The fact that in the X-ray structure this hydrogen bridge is not observed may be a consequence of the low resolution of this structure.

It is worth mentioning that these two residues belong to the already mentioned set of resistance mutations called TAMs that are associated with an increase in the level of removal of inhibitors (excision).

Up until now, it has not been possible experimentally to trap ATP or any other pyrophosphate donor bound to the binding site, that is, the *pyrophosphate donor pocket*. However, modeling of the ATP in the pyrophosphate donor pocket of RT has already been done[19] on the basis of the fact that the β- and γ-phosphates of ATP should be in the proper place to react with the inhibitor incorporated in the primer and that one of the TAMs, Thr215Tyr/Phe, improves ATP binding by providing stacking interactions with its base.

Looking at the positions of Lys219 and Asp67 in RT, it appears that they are located at the entrance of the proposed

Table 1. Most Frequent Hydrogen Bridges between the Enzyme and the dNTP/Inhibitors during the Simulations[a]

	E·dTTP				E·ddCTP				E·d4TTP			
acceptor	donor	% occup[b]	lifetime[c]	max occup[c,d]	donor	% occup[b]	lifetime[c]	max occup[c,d]	donor	% occup[b]	lifetime[c]	max occup[c,d]
O1G	113H	69.9	4.3	12.2	113H	43.4	3.7	7.8	113H	81.8	6.6	15
					114H	14.3	1.8	1.8	65HZ2	36.5	14.0	37.8
O2G	65HZ2	54.0	26.3	51.8					65HZ2	49.3	15.4	57.8
	65HZ3	19.6	32.2	37.4								
	219HZ1	18.0	5.7	10.4								
	219HZ2	32.9	10.0	43.6								
	219HZ3	31.1	9.0	32.2								
O1B					72HH21	23.9	1.7	3.2	72HH21	13.1	2.4	12.0
O2B	114H	9.5	1.2	0.8	65HZ1	11.6	5.6	10	114H	12.9	1.2	1.0
					65HZ2	19.7	5.9	9.2				
					65HZ3	41.5	7.2	11.2				
O2A	219HZ1	16.2	3.6	5.2					72HH12	13.0	4.8	5.0
	72HH12	14.0	7.3	12.6					72HH22	29.0	3.9	9.4
	72HH22	47.4	4.2	12.4								
O3A									72HH22	12.0	2.3	3.2
O3′	151HE22	24.5	2.2	6.2								
O4′					72HH12	67.6	3.5	6.8				
					72HH22	23.2	1.7	4.8				
O5′					72HH22	51.0	2.5	8.8				
N1					72HH12	49.2	2.4	2.2				
O2					151HE22	76.7	6.6	19.4	151HE22	85.1	17.8	21.0
O4	66HZ3	10.7	5.1	6.2								

[a] The length of the hydrogen bonds was not included because they range, in all cases, in the 2.8−2.9 Å interval. [b] Percentage of time the hydrogen bond is formed during the simulation [c] Given in picoseconds. [d] Maximum consecutive time the bond is formed.

pyrophosphate donor pocket. It can be hypothesized that their influence in excision can be regarded as a consequence of their interference with ATP binding or with the proper placement of the ATP triphosphate for productive excision.

3. Molecular Basis for the Multiresistance of the Gln151Met Mutant. During the simulations and regarding the dNTP binding site, we can only observe a hydrogen bridge between the 3′-OH on the ribose of the nucleoside and an amide hydrogen of Gln151. In the crystallographic structure of the RT·p/t·dTTP complex,[32] this hydrogen bridge is not observed because the side chain of Gln151 is in a conformation in which the carbonyl group is oriented toward the 3′-oxygen atom, this may be a consequence of the low resolution of the X-ray structure. Recently, kinetic evidence has also given support to the existence of this interaction.[33] In the inhibitors, which lack the 3′-hydroxyl group, this interaction is substituted by a hydrogen bridge of Gln151 with an oxygen atom of the base (O2) (Figure 2, Table 1).

The mutation of Gln151 for methionine, Gln151Met, confers low level resistance to AZT, ddI, ddC, and d4T,[34−36] but its combination with Ala62Val, Val75Ile, Phe77Leu, Phe116Tyr results in up to more than 100-fold resistance to AZT, ddI, ddC, and d4T and low cross resistance to 3TC.[35,37,38]

In these inhibitors, because they lack the 3′-hydroxyl group, Gln151 could engage in a hydrogen bridge with an oxygen atom from the base, as observed here with ddCTP and d4TTP. This is actually made possible due to the absence of the strong intramolecular ionic hydrogen bond between the 3′-OH and a β-phosphate oxygen atom of the triphosphate, which allows the ribose moiety of the inhibitor to stay more planar (in relation to the normal substrate) allowing the base to come closer to Gln151 (Figure 4). Consequently, the Gln151 mutation should further displace the inhibitors from the correct placement for catalysis because Gln151 is closer to their base. Because all the inhibitors lack the 3′-OH, the ubiquity of this mutation in causing resistance to NRTIs is understandable.

Additionally, in a previous article,[11] by observing the location of Ala62Val, Val75Ile, Phe77Leu, Phe116Tyr in the crystallographic structure 1RTD, we noticed that these residues were

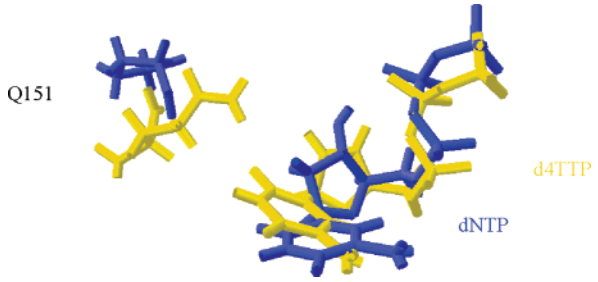

Figure 4. The d4TTP and Gln151 of the RT·p/t·d4TTP complex (yellow) and dNTP and Gln151 of the RT·p/t·dNTP complex (blue). As can be seen in the complex with the inhibitor, the base is closer to Gln151 than in the dNTP complex. The figure was obtained from the superposition of the α-carbons of the average structures (production runs).

positioned above the substrate and template bases. We proposed that they could create a hydrophobic cavity for the bases that contributes to the correct placement of the substrate in relation to the p/t. The two actions concerned, that is, the displacement of the substrate/inhibitor promoted by Met151 added to the changes in the substrate/inhibitor and template base pockets, should be responsible for the high level of resistance shown by the mutants.

4. Role of Lys65 and Arg72 in the Development of Resistance. Important hydrogen bridges of the nucleoside/analogues with the enzyme are established with residues 65 and 72 (Figures 2 and 3, Table 1). Both these residues are located in the fingers domain. Their interaction with the dTTP has been pointed out to promote the closing of the finger tips, a fundamental conformational change required for catalysis.[32]

From mutational studies, it is known that the Lys65Arg mutation is mainly associated with resistance to ABC, ddI, ddC, and PMPA.[34,37,39] The level of resistance provided by Lys65Arg to ddNTPs is moderate (<12 fold).[12,40]

The resistance conferred by this substitution to ddNTPs was previously proposed to be the result of the absence of the essential intramolecular bond between the lacking 3′-OH and one of the β-phosphate oxygens of the NRTIs. It was proposed

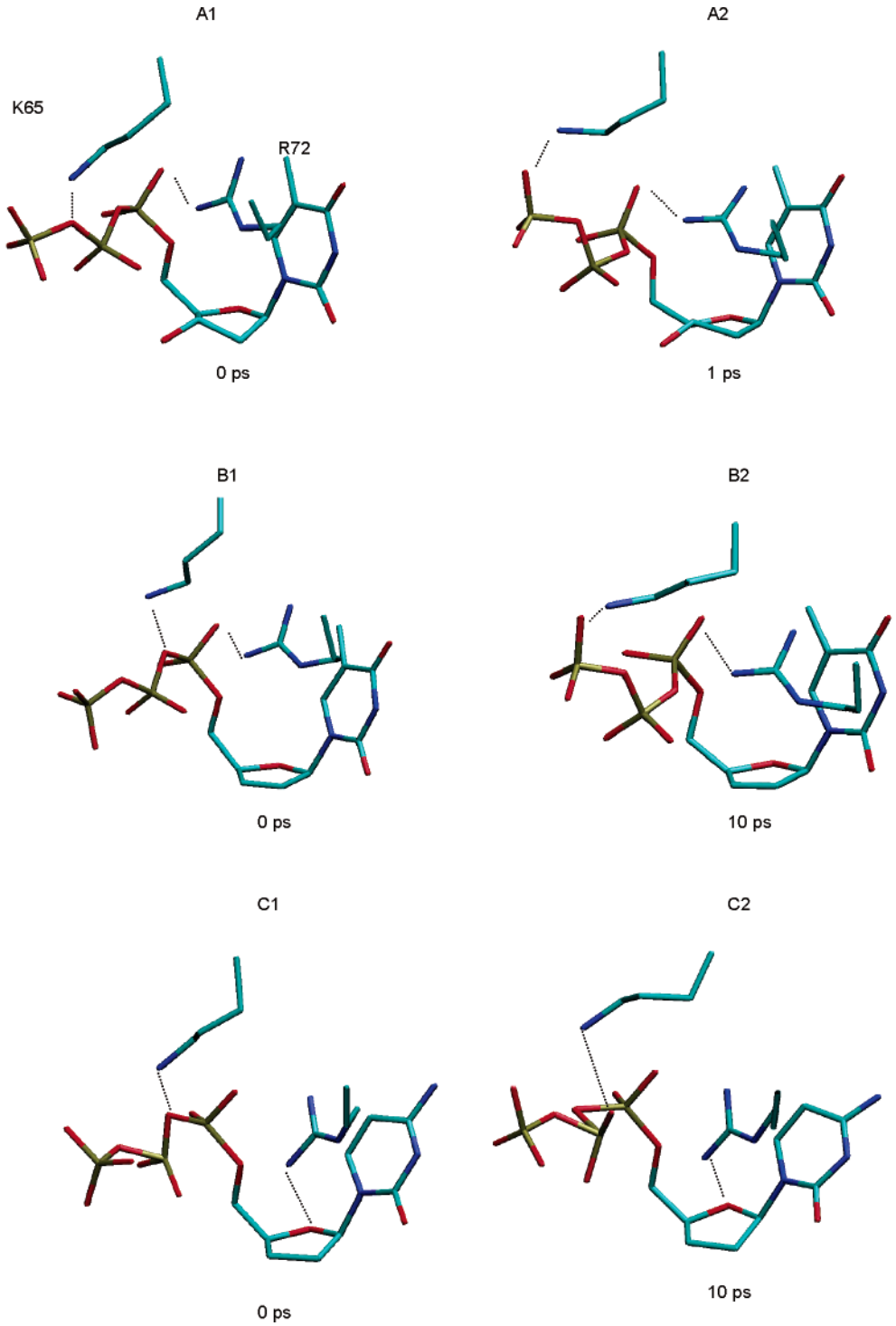

Figure 5. The substrate/inhibitor and the two finger tip residues (Lys65 and R62) in the dNTP binding site during the first picoseconds of simulation: (A) dNTP; (B) d4TTP; (C) ddCTP. The lack of an essential intramolecular interaction between one oxygen of the β-phosphate and the 3′-position of the ribose moiety of ddCTP results in a differential pattern of interactions between the enzyme finger tip residues and the inhibitor in relation to d4TTP and dNTP. This different pattern of interactions results in a displacement of the α-phosphate from the correct placement for catalysis and consequently in discrimination. All the dihedral rotations occur in the first picoseconds of simulation after the releasing of the restraints.

that in the absence of such bond, catalysis was impaired irrespective of which amino acid is present at position 65. When Lys65Arg and the normal substrate are present, the intramolecular bond of the substrate stabilizes the position of the α-phosphate. When the intramolecular bond is absent (ddNTPS) and Lys65Arg is present, Lys65Arg further displaces the α-phosphate from a correct alignment for catalysis.[14] However, this hypothesis does not explain why d4TTP (which lacks the 3′-hydroxyl group) is insensitive to the Lys65Arg mutation.

Observing our data (Table 1), we can see that for ddCTP the more permanent hydrogen bridge that Lys65 establishes is with an oxygen of the β-phosphate. This interaction is possible because the triphosphate moiety of this inhibitor is in a different conformation in relation to both the normal substrate and d4TTP. Consequently, the Lys65Arg mutation should displace the inhibitor ddCTP more than the normal substrate, consistent with the above-mentioned hypothesis. Even more interestingly, in the inhibitor d4TTP, the more permanent hydrogen bridge

formed by Lys65 is with the oxygen atoms of the γ-phosphate, a pattern it shares with the substrate. The main reason for this behavior is the existence of the fundamental intramolecular hydrogen bridge between the 3′-position of d4TTP and the β-phosphate. Even though d4TTP lacks the 3-hydroxyl group, the sp^2 proton is polar enough to keep such an essential intramolecular interaction and to keep its triphosphate in the same conformation as the substrate. In this way, we can understand, in a more general fashion, the appearance of resistance in the Lys65 mutants. Resistance occurs when the triphosphate has an incorrect conformation for incorporation. To have the correct conformation an essential hydrogen bridge between the 3′-position of the substrate/inhibitors and the β-phosphate must be present. This hydrogen bond can be established not only with a 3′-hydroxyl group but also with other groups at the 3′-position, given that they possess the necessary polarity and stereochemistry.

Regarding residue 72, this residue is evolutionarily conserved and intolerant to substitution, and hence, it should have an essential role in polymerase activity.[41,42] In all the simulations, this residue establishes hydrogen bridges with the substrate/inhibitor (Figure 2, Table 1). Curiously, another case of multinucleoside resistance is a family of insertion mutations between codons 67 and 70 that can cause resistance to ddI, 3TC, d4T, ddC, and AZT.[20] These mutations usually develop against a background of resistance to AZT. It is highly probable that an insertion between the mentioned residues results in a displacement of residue 72, and the displacement of this fundamental residue results in a displacement of the analogue.

5. The Fundamental Intramolecular Hydrogen Bond between the β-Phosphate and the 3′-Position of the Substrate/Inhibitor. One of the important results of the MD simulations consists of the different pattern of internal hydrogen bridges in the two inhibitors. In both dNTP and d4TTP, but not in ddCTP, the β-phosphate oxygen is involved in hydrogen bonding to the 3′-position. This difference sheds some light on the molecular causes of the inefficient incorporation of ddCTP compared with d4TTP or with the normal substrate. It seems reasonable to hypothesize that the intramolecular interaction between the oxygen of the β-phosphate and the group in the 3′-position of the ribose is fundamental for the correct placement of the nucleoside/analogue in relation to the primer. In the normal substrate, the bending of the β-phosphate toward the 3′ of the ribose is due to the intramolecular ionic hydrogen bridge between the 3′-OH group and one of the oxygens of the β-phosphate. In d4TTP, the more acidic hydrogen of the sp^2 carbon (in relation to an sp^3 carbon hydrogen as the one in ddCTP) at the 3′-position could in principle engage in an ion−dipole interaction with one of the oxygens of the β-phosphate; this interaction should allow the triphosphate of this inhibitor to adopt a conformation more similar to the one of the normal substrate. In contrast, the inhibitor ddCTP does not have any group in the 3′-position that could establish some kind of molecular interaction with the oxygens of the β-phosphate. Consequently, in ddCTP, due to the lack of this essential interaction, the β-phosphate oxygens engage in hydrogen bridges with Lys65 and Arg72 (Figure 3), and these last interactions result in a change in the conformation of the triphosphate (Figure 4) that can ultimately be responsible for the decrease in the efficiency of incorporation of this analogue.

To test this hypothesis, we have analyzed in more detail what happens during the first picoseconds of simulation (Figure 5). For the complex E·p/t·dTTP, the finger tip residue Lys65 establishes a hydrogen bridge with the O3B ester oxygen atom

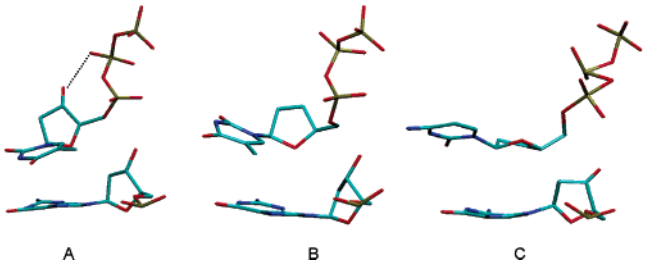

Figure 6. Position of the nucleoside and analogues in relation to the primer before the catalytic step: (A) dTTP; (B) d4TTP; (C) ddCTP. The different pattern of hydrogen bridges for ddCTP results in a modification of the conformation and an unfavorable placement of the α-phosphate of the inhibitor in relation to the primer for catalysis. The distances between the O3′ atom and the α-phosphate group are 3.25 Å for the dNTP, 3.10 Å for d4TTP, and 4.10 Å for ddCTP.

(Figure 5, panel A1). During the simulation, the side chain of this lysine is attracted to the more electronegative oxygen atom of the γ-phosphate (Figure 5, panel A2). For both inhibitors, at the beginning of the simulation, Lys65 establishes a hydrogen bridge with the O3A ester oxygen atom (Figure 5, panels B1 and C1). On the other hand, for d4TTP, after a few picoseconds the lysine starts to interact with the γ-phosphate oxygens as it happens with the normal substrate (Figure 5, panel B2; compare with panel A2). However, for ddCTP, the interaction moves to a β-phosphate oxygen atom (Figure 5, panel C2). The chemical explanation for this is that for ddCTP the lack of the interaction between the β-phosphate oxygen and the group at the 3′-position of the ribose moiety allows the anticlockwise rotation of the O5′−PA−O3A−PB dihedral in such a way that the β-phosphate oxygen can engage in a hydrogen bridge with the lysine residue. This rotation originates a change in the conformation of the triphosphate and the departure of the α-phosphate from the correct placement for catalysis to proceed (Figure 6).

For both the normal substrate and d4TTP, the interaction between the group in the 3′-position and the oxygen of the β-phosphate in the form of an ion−dipole interaction (in d4TTP this is due to the more acidic character of the hydrogen attached to the sp^2 carbon) does not allow the anticlockwise rotation of the dihedral, and hence the α-phosphate stays in the right place for catalysis to proceed (Figure 6).

In previous studies, in which the kinetic constants for incorporation in DNA/RNA chains were measured, the following values of incorporation efficiency were determined as follows: $1.8 \pm 0.2\ \mu M^{-1}\ s^{-1}$ for d4TTP and $2.1 \pm 0.4\ \mu M^{-1}\ s^{-1}$ for dTTP;[43] $1.73\ \mu M^{-1}\ s^{-1}$ for AZTTP and $2.5\ \mu M^{-1}\ s^{-1}$ for dTTP.[44] For cytosine analogues, the values of 0.0051 and $0.0013\ \mu M^{-1}\ s^{-1}$ were measured for ddCTP and (−)3TC-TP, respectively; for the normal substrate, dCTP, they measured a value of $0.080\ \mu M^{-1}\ s^{-1}$.[45] From these values, it can be concluded that d4TTP and AZTTP have incorporation efficiencies in WT RT similar to that of dTTP. In contrast, ddCTP presents a much smaller value of incorporation efficiency than its natural counterpart, dCTP.

Our results also point out that ddCTP should have *per se* a decreased efficiency of incorporation, and therefore, it seems reasonable to expect that the mutations contribute even more to decrease the efficiency of incorporation of the analogue in relation to the normal nucleosides. For example, in the Lys65Arg mutation, the bulky side chain of arginine with three hydrogen donors should contribute to an even more pronounced conformational change of the triphosphate moiety and hence to a larger displacement of the α-phosphate from the correct position for catalysis.

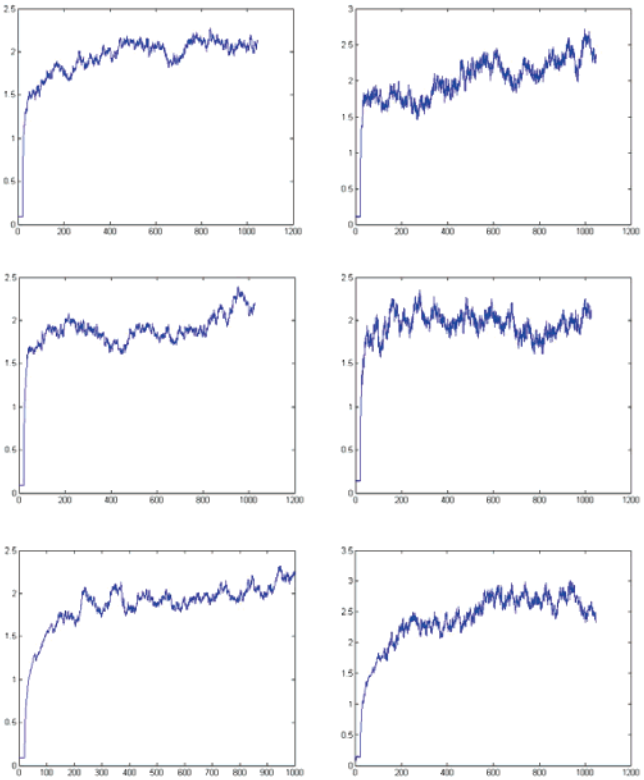

Figure 7. RMSD for the enzyme (left) and p/t (right) of the complexes E·p/t·dTTP (top), E·p/t·d4TTP (middle), and E·p/t·ddCTP (bottom).

In addition, other NRTIs such as ddI and 3TC, for which RT is resistant by discrimination at the level of incorporation, do not have any partial positively charged group at the 3′-position. ABC is an exception because it also has a more acidic sp^2 hydrogen. However this inhibitor has an extremely bulky substituted base that *per se* should be responsible for a large displacement of the inhibitor from the optimal position in relation to the primer for catalysis to proceed.

Conclusion

In this work, we performed three different simulations of WT RT; in one of them, we studied the interactions established between the N site residues and the normal substrate. In the other two, we studied the interactions of the N site residues with two inhibitors, d4TTP and ddCTP. These studies proved very important to elucidate on the development of resistance by RT to the antiretroviral drugs NRTIs.

One important observation is that of a new hydrogen bridge between the dNTP and a surface residue of the palm, Lys219, which is also involved in a salt bridge with the fingertip residue Asp67. RT mutants in these residues display increased levels of primer unblocking (excision). Looking at their position in the RT structure, these residues seem to be located at the entrance of the identified ATP binding site, which suggests that their mutation could favor ATP binding. However, further studies are necessary to prove this hypothesis.

Regarding residue Gln151, whereas with the normal substrate Gln151 is able to establish an interaction with the 3′-oxygen atom of the ribose moiety, in the presence of inhibitors this interaction occurs with an oxygen atom of the base because the absence of the 3′-OH in the inhibitors allows their base to came closer to Gln151. Consequently, when the mutation Gln151Met occurs together with Ala62Val, Val75Ile, Phe77Leu, and Phe116Tyr, the inhibitors should be more displaced from the correct placement for catalysis than the normal nucleotide.

Furthermore, based on the different pattern of hydrogen bridges between the fingertip residues of the enzyme (Lys65 and Arg72) and the triphosphate moieties of the normal nucleoside and d4TTP and ddCTP, two highly similar inhibitors for which RT presents reduced susceptibility by different mechanisms (discrimination at binding or incorporation and excision), we are able to suggest a general explanation for discrimination at the level of incorporation. Previous studies in which the relative incorporation of NRTIs and dNTP were compared have shown that WT HIV-1 RT barely discriminates between dTTP and AZTTP[44,46] or d4TTP.[43] In contrast, pre-steady-state kinetics showed that WT HIV-1 RT very efficiently discriminates against ddCTP on a DNA template.[45] From our study, we can now propose that the poor incorporation properties of ddCTP seem to come from the lack of a polar 3′-group, able to engage in an ion−dipole interaction with a β-phosphate oxygen of the triphosphate moiety, which results in a modification of the conformation of the triphosphate moiety and consequently in a displacement of the α-phosphate from the correct position for catalysis. Discrimination at the level of incorporation seems to be the consequence of the absence of this fundamental intramolecular interaction between the 3′-position of the ribose moiety and an oxygen atom of the β-phosphate.

Methods

Structural Modeling. The p66 subdomain along with the DNA p/t and the two magnesium ions of the X-ray structure 1RTD[32] were merged with a previously modeled p51 subunit[47] to form the complete complex E·p/t·dNTP. The missing hydrogens were added with the LEAP module of the Amber8 suite of programs.[48] The NRTIs were placed in the dNTP binding site by superposition of the substrate/inhibitor bases followed by deletion of the dTTP present in the 1RTD X-ray structure. For ddC, the corresponding template base was substituted by a thymidine.

Molecular Dynamics. All energy minimizations and MD simulations were carried out using the Amber8 package.[48]

The systems were neutralized by adding 37 Na^+ ions. The structures were then solvated with an octahedral box of TIP3P waters with each box side at a distance of at least 15 Å from the protein. The parm99 force field[49] was used in all calculations. This force field lacks atomic charges for the inhibitors. Therefore, atomic point charges for ddCTP and d4TTP had to be previously calculated. Accordingly, a first geometry of the inhibitors d4TTP and ddCTP was built from the structure of the dTTP present in GaussView[50] and then optimized in vacuum and subsequently using a PCM solvent model (with dielectric constant of 80).[51] The B3LYP functional was used as implemented in the Gaussian03 molecular package.[50] The 6-31G(d) basis set was employed.

Atomic charges were fitted to the restrained electrostatic potential at a fine grid of points generated according to the Merz−Kollman method.[52,53] The charges were derived using an electrostatic potential calculated with the B3LYP functional using the 6-31+G-(d) basis set.

Geometry minimizations of the whole RT·p/t·substrate and RRT·p/t·inhibitor systems were then performed using molecular mechanics. We began by optimizing the geometry of the solvent and the ions maintaining the protein atoms constrained by harmonic restraints (using a force constant of 500 kcal mol^{-1} $Å^{-2}$). Then we released the constraints on the entire system, and performed 1500 steps of steepest descent followed by 1000 steps of conjugate gradient to release the bad contacts present in the initial system, that is, enzyme X-ray structure/docked inhibitor.

The MD simulations were performed using periodic boundary conditions. The previously minimized systems were initially equilibrated at 300 K for 20 ps in an *NVT* ensemble, using Langevin dynamics. Production simulations were performed at 300 K in an *NTP* ensemble using Langevin dynamics with a collision frequency

of 1.0 ps^{-1}. Constant pressure periodic boundary was used with an average pressure of 1 atm. Isotropic position scaling was used to maintain the pressure with a relaxation time of 2 ps. The time step was set to 2 fs. Shake constraints were applied to all bonds involving hydrogen. The particle mesh Ewald (PME) method was used to calculate the electrostatic interactions with a cutoff distance of 10 Å. The trajectories were saved every 100 steps for analysis, with a total duration of around 1000 ps.

The simulations were carried out in the 108-node Intel/AMD Cluster at the Theoretical and Computational Chemistry Group of the Universidade do Porto.

Root-Mean-Square Deviation (RMSD). We began by analyzing the RMSDs of the enzyme (α-carbons) and the p/t for the three complexes (Figure 7). The RMSD for the enzyme equilibrates after 200 ps and can be observed to be low (around 2 Å) during the entire simulation, which means that the structures are stable and reproduce correctly the crystallographic geometry. The RMSDs for the p/t were calculated on the basis of the P, O3′, O5′, C3′, C4′, and C5′ atoms; furthermore, because the p/t has a cohesive end, we only considered the double-stranded portion. The p/t shows a larger but acceptable RMSD.

Acknowledgment. We are grateful for the financial support from Fundação para a Ciência e a Tecnologia (Portugal) for the fellowship SFRH/BD/17845/2004 and from the National Foundation for Cancer Research (NFCR, USA).

References

(1) Telesnitsky, A.; Goff, S. P. In *Retroviruses*; Coffin, J. M., Hughes, S. H., Varmus, H. E., Eds.; Cold Spring Harbor Laboratory Press: Cold Spring Harbor, NY, 1997.

(2) Bebenek, K.; Abbotts, J.; Roberts, J. D.; Wilson, S. H.; Kunkel, T. A. Specificity and mechanism of error-prone replication by human immunodeficiency virus-1 reverse transcriptase. *J. Biol. Chem.* **1989**, *264*, 16948−16956.

(3) Coakley, E. P.; Gillis, J. M.; Hammer, S. M. Phenotypic and genotypic resistance patterns of HIV-1 isolates derived from individuals treated with didanosine and stavudine. *AIDS* **2000**, *14*, F9−F15.

(4) Lin, P. F.; Gonzalez, C. J.; Griffith, B.; Friedland, G.; Calvez, V.; Ferchal, F.; Schinazi, R. F.; Shepp, D. H.; Ashraf, A. B.; Wainberg, M. A.; Soriano, V.; Mellors, J. W.; Colonno, R. J. Stavudine resistance: An update on susceptibility following prolonged therapy. *Antiviral Ther.* **1999**, *4*, 21−28.

(5) Gu, Z.; Gao, Q.; Fang, H.; Salomon, H.; Parniak, M. A.; Goldberg, E.; Cameron, J.; Wainberg, M. A. Identification of a mutation at codon 65 in the IKKK motif of reverse transcriptase that encodes human immunodeficiency virus resistance to 2′,3′-dideoxycytidine and 2′,3′-dideoxy-3′-thiacytidine. *Antimicrob. Agents Chemother.* **1994**, *38*, 275−281.

(6) Zhang, D.; Caliendo, A. M.; Eron, J. J.; DeVore, K. M.; Kaplan, J. C.; Hirsch, M. S.; D'Aquila, R. T. Resistance to 2′,3′-dideoxycytidine conferred by a mutation in codon 65 of the human immunodeficiency virus type 1 reverse transcriptase. *Antimicrob. Agents Chemother.* **1994**, *38*, 282−287.

(7) St. Clair, M. H.; Martin, J. L.; Tudor-Williams, G.; Bach, M. C.; Vavro, C. L.; King, D. M.; Kellam, P.; Kemp, S. D.; Larder, B. A. Resistance to ddI and sensitivity to AZT induced by a mutation in HIV-1 reverse transcriptase. *Science* **1991**, *253*, 1557−1559.

(8) Gao, Q.; Gu, Z.; Parniak, M. A.; Cameron, J.; Cammack, N.; Boucher, C.; Wainberg, M. A. The same mutation that encodes low-level human immunodeficiency virus type 1 resistance to 2′,3′-dideoxyinosine and 2′,3′-dideoxycytidine confers high-level resistance to the (-) enantiomer of 2′,3′-dideoxy-3′-thiacytidine. *Antimicrob. Agents Chemother.* **1993**, *37*, 1390−1392.

(9) Schinazi, R. F.; Lloyd, R. M., Jr.; Nguyen, M. H.; Cannon, D. L.; McMillan, A.; Ilksoy, N.; Chu, C. K.; Liotta, D. C.; Bazmi, H. Z.; Mellors, J. W. Antiviral drug resistance mutations in human immunodeficiency virus type 1 reverse transcriptase occur in specific RNA structural regions. *Antimicrob. Agents Chemother.* **1993**, *37*, 875−881.

(10) Tisdale, M.; Kemp, S. D.; Parry, N. R.; Larder, B. A. Rapid in vitro selection of human immunodeficiency virus type 1 resistant to 3′-thiacytidine inhibitors due to a mutation in the YMDD region of reverse transcriptase. *Proc. Natl. Acad. Sci. U.S.A.* **1993**, *90*, 5653−5656.

(11) Carvalho, A. P.; Fernandes, P. A.; Ramos, M. J. Molecular insights into the mechanisms of HIV-1 reverse transcriptase resistance to nucleoside analogues. *Mini.-Rev. Med. Chem.* **2006**, *6*, 549−555.

(12) Balzarini, J. Suppression of resistance to drugs targeted to human immunodeficiency virus reverse transcriptase by combination therapy *Biochem. Pharm.* **1999**, *58*, 1.

(13) Selmi, B.; Boretto, J.; Navarro, J. M.; Sire, J.; Longhi, S.; Guerreiro, C.; Mulard, L.; Sarfati, S.; Canard, B. The valine-to-threonine 75 substitution in human immunodeficiency virus type 1 reverse transcriptase and its relation with stavudine resistance. *J. Mol. Biol.* **2001**, *276*, 13965−13974.

(14) Selmi, B.; Boretto, J.; Sarfati, S. R.; Guerreiro, C.; Canard, B. Mechanism-based suppression of dideoxynucleotide resistance by K65R human immunodeficiency virus reverse transcriptase using an alpha-boranophosphate nucleoside analogue. *J. Biol. Chem.* **2001**, *276*, 48466−48472.

(15) Sluis-Cremer, N.; Arion, D.; Parniak, M.A. Molecular mechanisms of HIV-1 resistance to nucleoside reverse transcriptase inhibitors (NRTIs). *Cell. Mol. Life Sci.* **2000**, *57*, 1408−1422.

(16) Arion, D.; Kaushik, N.; McCormick, S.; Borkow, G.; Parniak, M. A. Phenotypic mechanism of HIV-1 resistance to 3′-azido-3′-deoxythymidine (AZT): Increased polymerization processivity and enhanced sensitivity to pyrophosphate of the mutant viral reverse transcriptase. *Biochemistry* **1998**, *37*, 15908−15917.

(17) Meyer, P. R.; Matsura, S. E.; Mian, A. M.; So, A. G.; Scott, W. A. A mechanism of AZT resistance: An increase in nucleotide-dependent primer unblocking by mutant HIV-1 reverse transcriptase. *Mol. Cell* **1999**, *4*, 35−43.

(18) Naeger, L.; Margot, N.; Miller, M. ATP-dependent removal of nucleoside reverse transcriptase inhibitors by human immunodeficiency virus type 1 reverse transcriptase. *Antimicrob. Agents Chemother.* **2002**, *46*, 2179−2184.

(19) Boyer, P. L.; Sarafianos, S. G.; Arnold, E.; Hughes, S. H. Selective excision of AZTMP by drug-resistant human immunodeficiency virus reverse transcriptase. *J. Virol.* **2001**, *75*, 4832−4842.

(20) Boyer, P. L.; Sarafianos, S. G.; Arnold, E.; Hughes, S. H. Nucleoside analog resistance caused by insertions in the fingers of human immunodeficiency virus type 1 reverse transcriptase involves ATP-mediated excision. *J. Virol.* **2002**, *76*, 9143−9151.

(21) Boyer, P. L.; Sarafianos, S. G.; Arnold, E.; Hughes, S. H. The M184V mutation reduces the selective excision of zidovudine 5′-monophosphate (AZTMP) by the reverse transcriptase of human immunodeficiency virus type 1. *J. Virol.* **2002**, *76*, 3248−3256.

(22) Mas, A.; Parera, M.; Briones, C.; Soriano, V.; Martinez, M. A.; Domingo, E.; Menedez-Arias, L. Role of a dipeptide insertion between codons 69 and 70 of HIV-1 reverse transcriptase in the mechanism of AZT resistance. *EMBO J.* **2000**, *19*, 5752−5761.

(23) Meyer, P. R.; Matsuura, S. E.; So, A. G.; Scott, W. A. Unblocking of chain-terminated primer by HIV-1 reverse transcriptase through a nucleotide-dependent mechanism. *Proc. Natl. Acad. Sci. U.S.A.* **1998**, *95*, 13471−13476.

(24) Meyer, P. R.; Matsuura, S. E.; Schinazi, R. F.; So, A. G.; Scott, W. A. Differential removal of thymidine nucleotide analogues from blocked DNA chains by human immunodeficiency virus reverse transcriptase in the presence of physiological concentrations of 2′-deoxynucleoside triphosphates. *Antimicrob. Agents Chem.* **2000**, *44*, 3465−3472.

(25) Meyer, P. R.; Lennestrand, J.; Matsuura, S. E.; Larder, B. A.; Scott, W. A. Relationship between 3′-azido-3′-deoxythymidine resistance and primer unblocking activity in foscarnet-resistant mutants of human immunodeficiency virus type 1 reverse transcriptase. *J. Virol.* **2003**, *77*, 6127−6137.

(26) Arion, D.; Sluis-Cremer, N.; Parniak, M. A. Mechanism by which phosphonoformic acid resistance mutations restore 3′-azido-3′-deoxythymidine (AZT) sensitivity to AZT-resistant HIV-1 reverse transcriptase. *J. Biol. Chem.* **2000**, *275*, 9251−9255.

(27) Götte, M.; Arion, D.; Parniak, M. A.; Wainberg, M. A. The M184V mutation in the reverse transcriptase of human immunodeficiency virus type 1 impairs rescue of chain-terminated DNA synthesis. *J. Virol.* **2000**, *74*, 3579−3585.

(28) Krebs, R.; Immendorfer, U.; Thrall, S. H.; Wohrl, B. M.; Goody, R. S. Single-step kinetics of HIV-1 reverse transcriptase mutants responsible for virus resistance to nucleoside inhibitors zidovudine and 3-TC. *Biochemistry* **1997**, *36*, 10292−10300.

(29) Martin, J. L.; Wilson, J. E.; Haynes, R. L.; Furman, P. A. Mechanism of resistance of human immunodeficiency virus type 1 to 2′,3′-dideoxyinosine. *Proc. Natl. Acad. Sci. U.S.A.* **1993**, *90*, 6135−6139.

(30) Gu, Z.; Quan, Y.; Li, Z.; Arts, E. J.; Wainberg, M. A. Effects of non-nucleoside inhibitors of human immunodeficiency virus type 1 in cell-free recombinant reverse transcriptase assays. *J. Biol. Chem.* **1995**, *270*, 31046−31051.

(31) Isel, C.; Ehresmann, C.; Walter, P.; Ehresmann, B.; Marquet, R. The emergence of different resistance mechanisms toward nucleoside inhibitors is explained by the properties of the wild type HIV-1 reverse transcriptase. *J. Biol. Chem.* **2001**, *276*, 48725−48732.

(32) Huang, H.; Chopra, R.; Verdine, G. L.; Harrison, S. C. Structure of a covalently trapped catalytic complex of HIV-1 reverse transcriptase: Implications for drug resistance. *Science* **1998**, *282*, 1669−1675.
(33) Jamburuthugoda, V. K.; Guo, D.; Wedekind, J. E.; Kim, B. Kinetic evidence for interaction of human immunodeficiency virus type 1 reverse transcriptase with the 3′-OH of the incoming dTTP substrate. *Biochemistry* **2005**, *44*, 10635−10643.
(34) Shirasaka, T.; Klavlick, M. F.; Ueno, T.; et al. Emergence of human immunodeficiency virus type 1 variants with resistance to multiple dideoxynucleosides in patients receiving therapy with dideoxynucleosides. *Proc. Natl. Acad. Sci U.S.A.* **1995**, *92*, 2398−2402.
(35) Iversen, A. K.; Shafer, R. W.; Werly, K.; Winters, M. A.; Mullins, J. L.; Chesebro, B.; Merigan, T. C. Multidrug-resistant human immunodeficiency virus type 1 strains resulting from combination antiretroviral therapy *J. Virol.* **1996**, *70*, 1086−1090.
(36) Kavlick, M. F.; Wyvill, K.; Yarchoan, R.; Mitsuya, H. Emergence of multi-dideoxynucleoside-resistant human immunodeficiency virus type 1 variants, viral sequence variation, and disease progression in patients receiving antiretroviral chemotherapy. *J. Inf. Dis.* **1998**, *177*, 1506−1513.
(37) Ueno, T.; Shirasaka, T.; Mitsuya, H. Enzymatic characterization of human immunodeficiency virus type 1 reverse transcriptase resistant to multiple 2′,3′-dideoxynucleoside 5′-triphosphates. *J. Biol. Chem.* **1995**, *270*, 23605−23611.
(38) Garcia Lerma, J.; Schinazi, R. F.; Juodawlkis, A. S.; Soriano, V.; Lin, Y.; Tatti, K.; Rimland, D.; Folks, T. M.; Heneine, W. A rapid non-culture-based assay for clinical monitoring of phenotypic resistance of human immunodeficiency virus type 1 to lamivudine (3TC). *Antimicrob. Agents Chemother.* **1999**, *43*, 264−270.
(39) Roge, B. T.; Katezenstein, T. L.; Obel, N.; et al. K65R with and without S68: A new resistance profile in vivo detected in most patients failing abacavir, didanosine and stavudine. *Antivir. Ther.* **2003**, *8*, 173.
(40) Schinazi, R. F.; Larder, B. A.; Mellors, J. W. Mutations in retroviral genes associated with drug resistance. *Int. Antivir. News* **1996**, *4*, 95−107.
(41) Boyer, P. L.; Ferris, A. L.; Hughes, S. H. Mutational analysis of the fingers domain of human immunodeficiency virus type 1 reverse transcriptase. *J. Virol.* **1992**, *66*, 7533−7537.
(42) Kim, B.; Hathaway, T. R.; Loeb, L. A. Human immunodeficiency virus reverse transcriptase. Functional mutants obtained by random mutagenesis coupled with genetic selection in *Escherichia coli*. *J. Biol. Chem.* **1996**, *271*, 4872−4878.
(43) Vaccaro, J. A.; Parnell, K. M.; Terezakis, S. A.; Anderson, K. S. Mechanism of inhibition of the Human Immunodeficiency Virus Type 1 Reverse Transcriptase by d4TTP: An equivalent incorporation efficiency relative to the natural substrate dTTP. *Antimicrob. Agents Chemother.* **2000**, *44*, 217−221.
(44) Kerr, S. G.; Anderson, K. S. Pre-steady-state kinetic characterization of wild type and 3′-azido-3′-deoxythymidine (AZT) resistant human immunodeficiency virus type 1 reverse transcriptase: Implication of RNA directed DNA polymerization in the mechanism of AZT resistance. *Biochemistry* **1997**, *36*, 14064−14070.
(45) Feng, J. Y.; Anderson, K. S. Insights into the molecular mechanism of mitochondrial toxicity by AIDS drugs. *Biochemistry* **1999**, *38*, 55−63.
(46) Rigourd, M.; Lanchy, J. M.; Le Grice, S. F.; Ehresmann, B.; Ehresmann, C.; Marquet, R. Inhibition of the initiation of HIV-1 reverse transcription by 3′-azido-3′-deoxythymidine. Comparison with elongation. *J. Biol. Chem.* **2000**, *275*, 26944−26951.
(47) Carvalho, A. T. P.; Fernandes, P.A.; Ramos, M. J. Molecular dynamics model of unliganded HIV-1 reverse transcriptase. *Med. Chem. J.*, in press.
(48) Case, D. A.; Darden, T. A.; Cheatham, T. E.; Simmerling, C. L., III; Wang, J.; Duke, R. E.; Luo, R.; Merz, K. M.; Wang, B.; Pearlman, D. A.; Crowley, M.; Brozell, S.; Tsui, V.; Gohlke, H.; Mongan, J.; Hornak, V.; Cui, G.; Beroza, P.; Schafmeiste, r. C.; Caldwell, J. W.; Ross, W. S.; Kollman, P. A. *AMBER 8*; University of California: San Francisco, 2004.
(49) Cornell, W. D.; Cieplak, P.; Bayly, C. I.; Gould, I. R.; Merz, K. M. Jr.; Ferguson, D. M.; Spellmeyer, D. C.; Fox, T.; Caldwell, J. W.; Kollman, P. A. A Second Generation Force Field for the Simulation of Proteins, Nucleic Acids, and Organic Molecules *J. Am. Chem. Soc*. **1995**, *117*, 5179−5197.
(50) Frisch, M. J.; Trucks, G. W.; Schlegel, H. B.; Scuseria, G. E.; Robb, M. A.; Cheeseman, J. R.; Montgomery, J. A., Jr.; Vreven, T.; Kudin, K. N.; Burant, J. C.; Millam, J. M.; Iyengar, S. S.; Tomasi, J.; Barone, V.; Mennucci, B.; Cossi, M.; Scalmani, G.; Rega, N.; Petersson, G. A.; Nakatsuji, H.; Hada, M.; Ehara, M.; Toyota, K.; Fukuda, R.; Hasegawa, J.; Ishida, M.; Nakajima, T.; Honda, Y.; Kitao, O.; Nakai, H.; Klene, M.; Li, X.; Knox, J. E.; Hratchian, H. P.; Cross, J. B.; Bakken, V.; Adamo, C.; Jaramillo, J.; Gomperts, R.; Stratmann, R. E.; Yazyev, O.; Austin, A. J.; Cammi, R.; Pomelli, C.; Ochterski, J. W.; Ayala, P. Y.; Morokuma, K.; Voth, G. A.; Salvador, P.; Dannenberg, J. J.; Zakrzewski, V. G.; Dapprich, S.; Daniels, A. D.; Strain, M. C.; Farkas, O.; Malick, D. K.; Rabuck, A. D.; Raghavachari, K.; Foresman, J. B.; Ortiz, J. V.; Cui, Q.; Baboul, A. G.; Clifford, S.; Cioslowski, J.; Stefanov, B. B.; Liu, G.; Liashenko, A.; Piskorz, P.; Komaromi, I.; Martin, R. L.; Fox, D. J.; Keith, T.; Al-Laham, M. A.; Peng, C. Y.; Nanayakkara, A.; Challacombe, M.; Gill, P. M. W.; Johnson, B.; Chen, W.; Wong, M. W.; Gonzalez, C.; Pople, J. A. *Gaussian 03*, revision B.04; Gaussian, Inc.: Wallingford, CT, 2004.
(51) Cammi, R.; Mennucci, B.; Tomasi, J. Fast evaluation of geometries and properties of excited molecules in solution: A Tamm−Dancoff model with application to 4-dimethylaminobenzonitrile. *J. Phys. Chem.* A. **2000**, *104*, 5631−5637.
(52) Singh, U. C.; Kollman, P. A. An approach to computing electrostatic charges for molecules. *J. Comput. Chem.* **1984**, *5*, 129−145.
(53) Besler, B. H.; Merz, K. H.; Kollman, P. A. Atomic charges derived from semiempirical methods. *J. Comput. Chem.* **1990**, *11*, 431−439.

JM060698C